PROBING MOLECULAR ATTACHMENTS TO CELL SURFACE RECEPTORS: Image of Stochastic Bonding and Rupture Processes

EVAN EVANS and KEN RITCHIE
Departments of Physics and Pathology
University of British Columbia
Vancouver, B.C. Canada V6T IW5

ABSTRACT. Biological cell adhesion involves specific-molecular bonds to sparsely distributed surface receptors. Thus, physical tests of adhesion probe rupture of a discrete set of molecular attachments which, if sufficiently small, is expected to expose failure of individual molecular complexes. However, in recent tests using ultrasensitive techniques, measurements of attachment strength have been broadly distributed even when single molecular attachments are present. It appears that the distributed force response images an underlying stochastic character of molecular failure. To extract the submicroscopic determinants of rupture, the distribution of attachment strengths must be correlated with convolutions of random process models for molecular bonding and failure. Unexpectedly, this analysis shows that peaks in strength distributions occur as a consequence of progressive force loading - not solely because of discrete attachment! Using results from recent tests of monoclonal antibody attachments to red cell membrane receptors, we demonstrate the subtle indeterminancies inherent to probing molecular bonds in biological adhesion and outline a procedure for statistical deconvolution of rupture force data.

1. Introduction

Adhesion between biological interfaces is important in many fields of science and technology. From extensive studies in biology, much is known about the phenomenological and biochemical features of adhesion [1-2]. However, little is known about the physical actions that mediate bonding and govern strength of attachment. Recognizing the need to expose actions at the submicroscopic level, many research groups are employing ultrasensitive force techniques to probe extremely small regions of adhesive contact between surfaces bearing biological molecules [3-7]. Characteristic of macromolecular bonds, attachment between interfaces occurs at short range - essentially through direct molecular contact - with little evidence of long range attraction. As such, adhesive contact involves multiple point links between surfaces. Naively then, we expect that the forces necessary to separate small regions of contact should group about distinct values which represent rupture of discrete molecular linkages. But, as we will illustrate with experimental data from tests using monoclonal antibodies to well-defined surface receptors, forces to rupture submicroscopic areas of adhesive contact are spread over a broad range with only weak indications of discrete forces. Since experimental resolution is not in question, the distribution in attachment strength must reflect the stochastic nature of both initial bonding and subsequent detachment processes at the molecular level. Therefore, the challenge is to extract physical properties of single molecular attachments in the face of inherent uncertainty. We will examine the impact of molecular level indeterminancy on macroscopic measurements of detachment force using a general statistical model for dynamic failure of an attachment under external load. The results show that application of force over finite time leads to a peak in the distribution of rupture force and the shape of the distribution is regulated subtlely by the form of the intermolecular potential near failure. When more than one molecular attachment is involved, the situation becomes extremely complex because both the statistical properties of the assembly process and partition of the load amongst the sites must be considered.

2. Strength of Molecular Attachments to Cell Surface Receptors

The strength of molecular attachment to a cell membrane receptor is determined by the weakest component of the complex: i.e. the ligand-receptor bond or anchorage of the receptor to the membrane. Thus, for high-affinity ligands like antibodies, cohesive linkage of the receptor to the membrane is expected to dominate adhesion strength. Because of its fluid cytoplasm and lack of internal structure, the mammalian red blood cell has been chosen as a prototype to test the hypothesis that physical coupling between cell surface receptors and membrane components governs strength of intersurface attachments. In the red cell, the membrane is a composite of fluid lipid bilayer (with cholesterol, glycolipids, and glycoproteins embedded as solutes) supported by a filamentous protein scaffolding - referred to as the membrane cytoskeleton. Using in vitro binding analyses after chemical digestion, biochemists have categorized red cell surface receptors according to relative affinity for the membrane cytoskeleton, lipid bilayer, or both [8-9]. Fortunately, monoclonal antibodies (Mab) have been raised against many red cell receptors, which provides a means of strongly liganding these receptors to physical probes. Here, the differential effect of cytoskeletal coupling is demonstrated by comparing results obtained for strength of attachment to two distinct receptors in the red cell membrane: i.e. glycophorins A and C [10]. Both glycoproteins have a single membrane-spanning hydrophobic peptide sequence with modestsize cytoplasmic domains; however, only glycophorin C shows an affinity for the cytoskeleton in binding studies. In previous work [11], we found that glycophorin A was weakly anchored to the membrane with a strength of attachment equal to that obtained for attachment to glycolipid receptors, - indicating linkage only to the lipid bilayer. However, as will be shown, the strengths of attachments to glycophorin C receptors exhibit two broad populations with a preponderance of much stronger forces indicating linkages to the cytoskeleton. [Note: in the glycophorin A studies, it was clear that the ligand receptor bond was much stronger than the strength of receptor linkage to the membrane; but this may not be the case when there is strong coupling to cytoskeletal structure.]

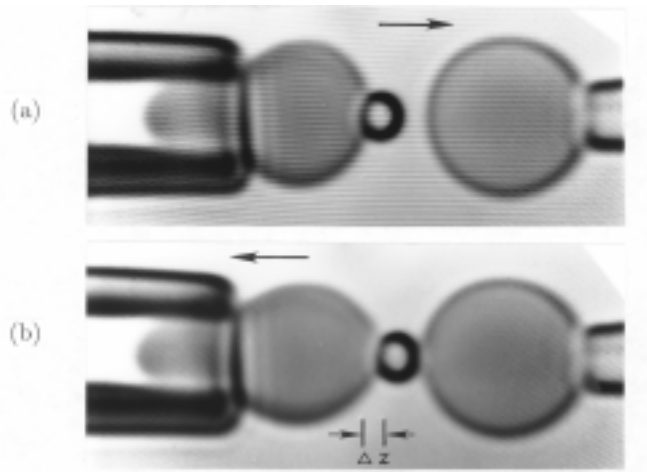

Figure 1. Videomicrographs of a red cell transducer-probe assembly (a) approaching a red cell test surface and (b) withdrawing from the surface following point contact. The extension in length Δz of the transducer capsule yields the force applied to molecular attachments between antibodies on the probe and receptors native to the test surface.

In order to probe attachments to single receptors, we have developed an ultrasensitive-tunable transducer that can measure forces over a range from 10^{-2} pN up to 10^{3} pN characteristic of weak covalent bonds [7]. The transducer assembly is simply a microbead probe *glued* to a pressurized membrane capsule which, for the experiments to be discussed here, was a human red blood cell

(demonstrated in Fig. 1). The *spring constant* k_f of the transducer is given by the tension in the capsule membrane set by suction pressure P in the holding micropipet - i.e. $k_f \sim P \cdot R_p$ where R_p is the pipet radius. The small microbead is chemically conjugated with both a dense molecular *glue* for attachment to the membrane of the transducer capsule and a sparse distribution of specific ligands for bonding to receptors in the test surface - e.g. the membrane of another red cell. By reducing the amount of ligand specific to the receptors in the test surface, we reach a condition where repeated attempts to make point contact between the probe and the surface results in infrequent attachments. These attempts are performed by precise sequences of micromechanical translation to/from the test surface over a distance of ~ 1 μm. An attachment is exposed when a small extension of the capsule Δz occurs as the transducer is withdrawn from the point contact. The strength of attachment is given by the transducer extension at rupture - i.e. $f = k_f \cdot \Delta z$.

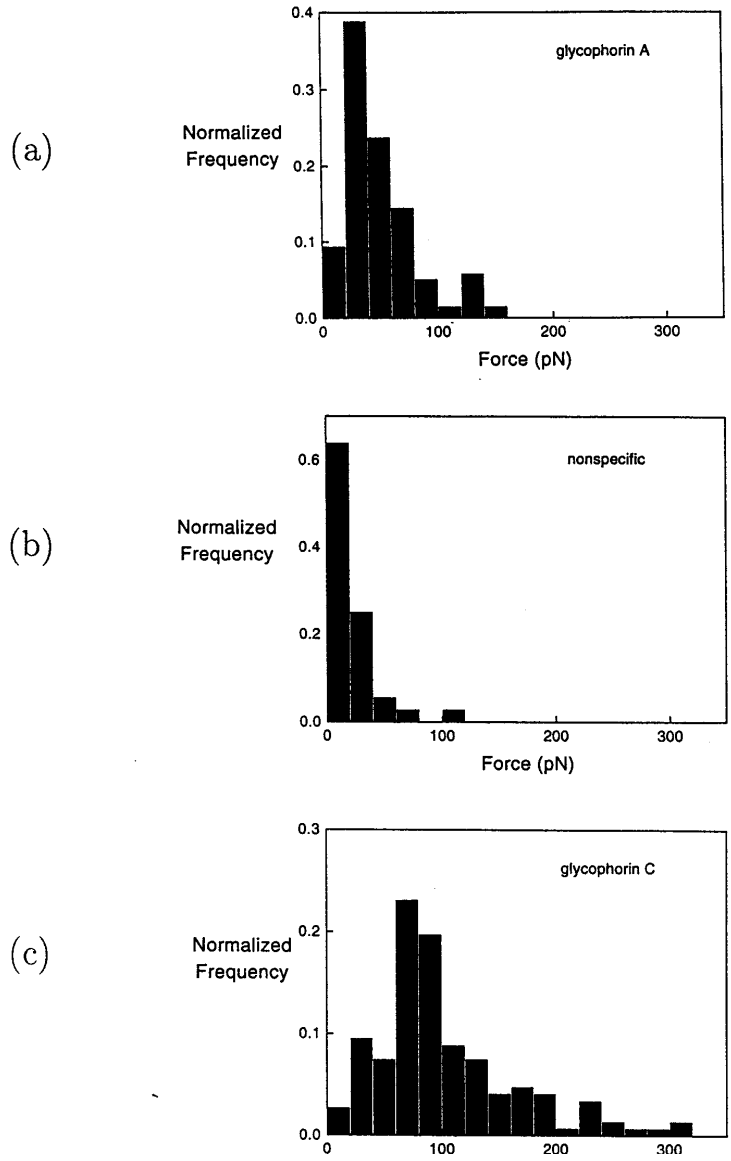

Figure 2. Forces required to rupture submicroscopic-point attachments between a transducer probe and red cell test surfaces when the probe was conjugated with (a) an IgG antibody to glycophorin A receptors, (b) a lectin indifferent to the blood type of the test red cell, and (c) an IgG antibody to glycophorin C receptors. Note: each distribution represents about 50 attachments that formed out of several hundred attempts.

Using this technique and microbeads conjugated with monoclonal antibodies, we have probed the strength of attachments made to glycophorins A and C in membranes of test red cells [10]. Nonspecific attachments were exposed by conjugating the probe with a lectin indifferent to the blood type of the test red cell. Strengths of attachments are plotted in Figs. 2a and 2c for probes specific to glycophorins A and Q results for nonspecific attachments are presented in Fig. 2b. In these tests, the resolution in the force measurement was limited to 1 pN by video discrimination of the transducer extension. [Note: resolution of the force can be significantly improved when more sensitive optical methods are employed to measure displacements of the probe - see ref. 7.] As shown in Fig. 2, nonspecific attachments were weak with most of the rupture forces below 20 pN. Attachments to glycophorin A receptors were clearly stronger with a most frequent rupture force around 20 - 30 pN. However, attachments to glycophorin C yielded a bimodal distribution with a second peak at larger forces around 80 - 90 pN. The bimodal distribution is consistent with observations using fluorescence recovery after photobleaching FRAP techniques that there are laterally mobile and immobile populations of glycophorin C in red cell membranes [14]. Presumably, mobile receptors are anchored only to the lipid bilayer whereas immobile receptors are also coupled to the cytoskeleton. Even with the obvious appearance of stronger attachments to glycophorin C than to glycophorin A and a rationale for the bimodal distribution of strengths, the spread of rupture forces about peaks in these distributions obscures the intrinsic properties of specific attachments. Therefore, we must consider the hidden indeterminancies associated with assembly and detachment processes at the molecular scale.

3. Stochastic Character of Adhesive Bonding and Contact Fracture

3.1 INITIAL BONDING

As emphasized, adhesive contact in biology involves direct molecular attachments between surfaces. When small regions bearing sparse numbers of receptors and ligands are brought into contact, the likelihood of adhesive bonding depends strongly on details of surface topography and conformational flexibility at the molecular level [12]. Consequently, it is not surprising that infrequent attachments occurred in the red cell experiments described in the previous section where surface densities of ligands and receptors were very low. Ideally, if adhesive molecules are randomly distributed and all attempts at assembly are the same, we expect that the probability of forming molecular attachments should follow a binomial distribution and, if infrequent, be represented as a Poisson distribution [13]. More subtle, not all attempts to form attachments may be equivalent. For example, if the surfaces fail to get sufficiently close during an attempt, the nonattachment event must be counted separate from events where the surfaces effectively touch but do not bond. The question is how to discriminate between these two events that appear the same to the observer? Clearly, the best method is to measure the distance between the surfaces; however, this is often not accessible experimentally. Therefore, as a practical solution, we introduce an indirect method based on treating *nonspecific* adhesion events as nonattachments. If specific and nonspecific attachment events can be properly distinguished, the mean probability of forming a single specific bond can be estimated along with the relative likelihood of forming multiple bonds. Then, stochastic features of assembly can be removed from the distribution of rupture strength to isolate the statistics of molecular failure. [Note: nonspecific adhesion appears to arise mainly from van der Waals attraction between the surfaces. For soft membrane interfaces of cells, this force is extremely weak because of steric repulsion and rapid attenuation of attraction between thin membranes at large separations [12]. For example, nonspecific attachments do not form after flexible red cell membranes touch in buffer. However, when solid beads touch red cells, small forces arise on separation that are not produced by specific ligands. Consistent with the data plotted in Fig. 2b, estimates of van der Waals force between a latex microsphere and a membrane show that the strength of attachment can easily reach ~ 10 pN if surfaces approach within 10 nm.]

To demonstrate this approach, we have taken the principal range of forces shown in Fig. 2b ($\leq$ 20 pN) as an estimator for nonspecific attachments in the red cell tests. Next, comparing the sample number found in this *nonspecific* bin with the number of attachments ruptured by larger forces, we

deduced average probabilities of forming specific attachments during assembly for each set of experiments shown in Figs. 2a and 2c. As mentioned, the subtle feature in Fig. 2c is that two different receptor populations seem to be associated with the same specific ligand - laterally mobile and immobile - as identified by measurements of surface diffusion [14]. Thus, separate probabilities of forming two specific attachments had to be considered for the data in Fig. 2c. To define these probabilities, we assumed that formation of a bond to either a mobile or immobile receptor was equally likely. As such, the ratio of average probabilities was defined by the ratio of mobile to immobile fractions known *a priori*. Following this simple procedure, distributions were predicted for the numbers of bonds involved in these attachments as shown in Figs. 3a and 3b. The reliability of this step in statistical deconvolution depends on success in detection of nonspecific attachments. When specific molecular bonds lead to much stronger attachments, many weak-nonspecific forces may escape detection. This seems to have been the case in tests of antibody attachments to glycophorin C receptors (cf. Fig. 2c). As will be discussed, optimal correlation of both statistical assembly *and* detachment processes with the data in Fig. 2c implies that the frequency of nonattachments was probably ten fold higher than detected and that the numbers of bonds in attachments were distributed more like Fig. 3c.

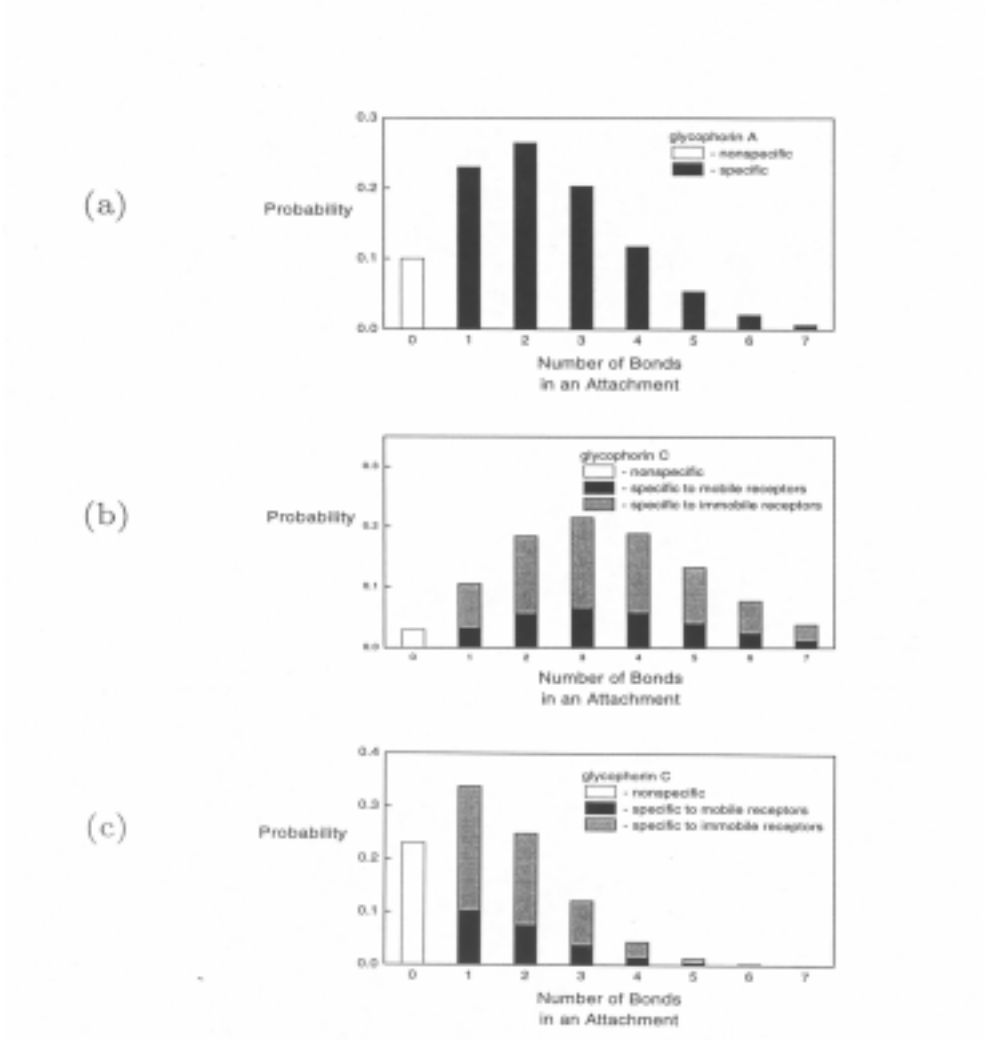

Figure 3. Numbers of bonds in attachments to glycophorin A and glycophorin C receptors derived from the data presented in Fig. 2. In (a) and (b), the distributions were predicted using the assumption that forces measured in the 0-20 pN range were nonspecific and represent the likelihood of *zero* bonds in an attachment. The distribution in (c) was found from optimal correlation of both statistical assembly and detachment processes allowing, the frequency of *zero* bonds to vary; the result in (a) was unaffected by this procedure.

3.2 SUBSEQUENT DETACHMENT

3.2.1 *Single Adhesive Bonds.* The next step is to introduce a stochastic model for the process of molecular detachment. Even for single bonds, detachment by force over finite times is a nonequilibrium process that can be difficult to predict theoretically. Moreover, an attachment site is a complex of molecular connections. Viewing covalent bonds as unbreakable, we immediately recognize two weak (noncovalent) links in an attachment: i.e. anchorage of the receptor to the material structure of the membrane and the ligand-receptor bond itself. Although rupture statistics reflect convolution over all possible mechanisms, we conceptualize failure as emanating from a single locus in the complex. Since application of force by mechanical techniques will occur over time periods that greatly exceed molecular relaxation times, the distribution of rupture strengths images a kinetic transition mediated by thermal excitations. Hence, the long-time *average* frequency of failure ν (#/time) is expected to be scaled by a Boltzmann-like factor [15],

$$\nu \sim e^{-(E-E_o)/k_BT}$$

that depends on the energy increase ($E - E_0$) imparted to the attachment by mechanical force; k_BT is the thermal energy. In general, dependence of the energy increase $\Delta E(f)$ on force is unknown and, moreover, will be strongly anharmonic at energies near E_0 where failure is imminent. Thus, for complex bonds that sustain some protracted level of force without immediate rupture, a more useful approximation is to represent the frequency of failure by a phenomenological relation [11-12],

$$\nu = \nu_o(f/f_o)^a$$

The exponent *a* characterizes the stiffness of the energy of activation in the domain of likely failure (i.e. within k_BT of E_0) where the force level is f_0 and the average rate of failure is ν_0. Qualitatively, exponents $a >> 1$ represent *brittle* bonds where rupture ensues precipitously as the applied force reaches f_0; but, exponents $a \sim 1$ represent *ductile* bonds that slowly increase their rate of failure as applied force exceeds f_0. Given the statistical law for rate of failure under load, the probability $p(t, f) \cdot dt$ for failure within a small interval dt around the observation time t decreases exponentially following a step application of force in proportion to the likelihood of *survival*, i.e.

$$p(t, f) = \nu \cdot e^{-\nu \cdot t}$$

Illustrated in Fig. 4a, larger forces simply lead to more rapid failure and distributions skewed to shorter times as expected. There is no distinct level of rupture force that decribes the most likely failure of an attachment! Hence, our original expectation of *quantized* rupture forces for molecular attachments seems to be naive and inconsistent with this simple physical picture. However, the analysis at this point is unrealistic since force is always applied progressively to an attachment - increasing at a finite rate over time until rupture. Therefore, we examine the case of a steady increase in load per time $\dot{f}$. Force and time become coupled so that the statistical distribution for failure depends only on the instantaneous force $f = \dot{f} \cdot t$,

$$p(f) \sim (f/\hat{f})^a \cdot e^{-(f/\hat{f})^{a+1}/a+1}$$

$$\hat{f} \equiv f_o/(a \cdot \nu_o t_f)^{1/a+1} \qquad t_f \equiv f_o/\dot{f}$$

and a characteristic experimental time $t_f = f_0 / \dot{f}$ to reach failure. As such, a natural scale for force $\hat{f}$ arises that defines a peak in the distribution. This gives the *appearance* of a quantized rupture strength for a single attachment; but clearly, it is the dynamic process of loading that gives rise to the distinct peak. As we see, the most likely force for rupture depends on experimental loading rate and does not scale precisely with the molecular rupture force f_0. However, since the fractional exponent $1/a+1$ is probably small (~1/3), the *apparent* rupture strength only changes weakly with the rate of loading. Likewise, since $a/a+1$ is close to unity, the apparent rupture strength scales approximately as the molecular force f_0. On the other hand, the stiffness of the molecular potential near failure plays an important role in the strength distribution. Illustrated in Fig. 4b, we see that the failure distribution for *ductile* bonds is broad whereas the distribution is narrow for *brittle* bonds. When recognized in experimental data, these signatures provide important clues to the character of the molecular-thermodynamic potential near rupture.

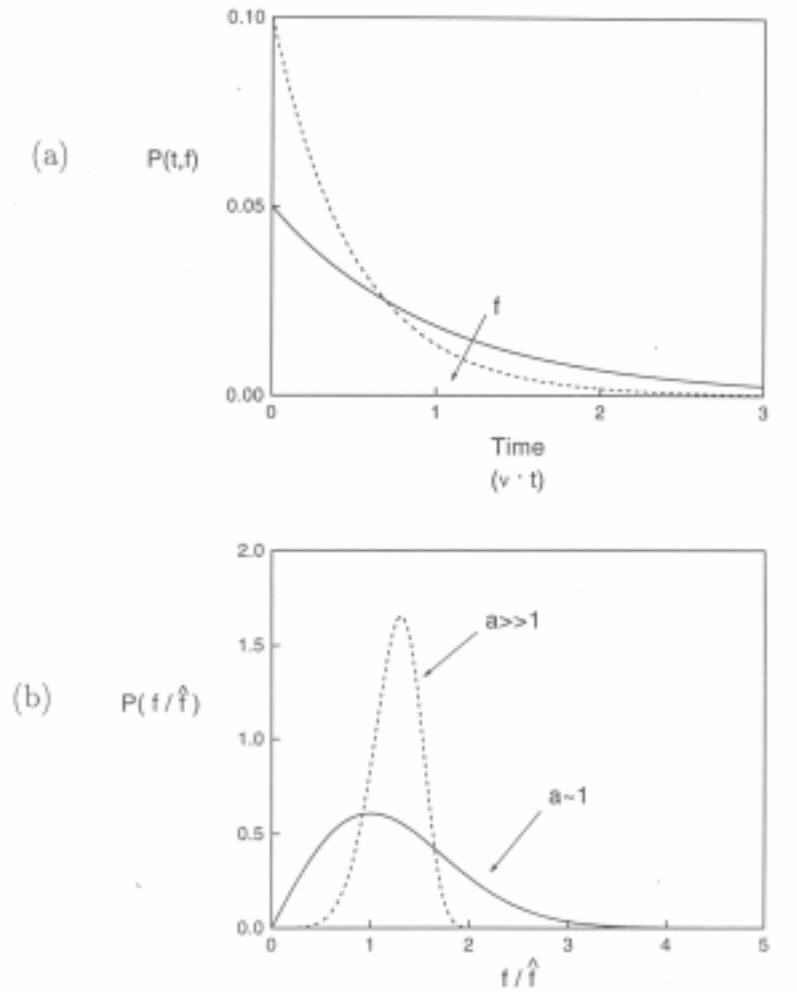

Figure 4. Illustrations of probability densities for failure of a single molecular attachment as functions of (a) increasing time following application of a constant force f and (b) steadily increasing force $f = \dot{f} \cdot t$ normalized by the most probable rupture force $\hat{f}$ defined in the text. The exponent a characterizes the dependence of frequency of failure on force, i.e. $\nu \sim (f / f_0)^a$.

3.2.2 *A Few Adhesive Bonds.* When contact areas are small and there are sparse numbers of ligands or

receptors, formation of multiple adhesive bonds on contact will be infrequent and should follow Poisson statistics. Based on these considerations, we conclude that one to three bonds were probed in the experiments described in Section 2 (c.f. Fig. 3). Even so, it is important to consider the consequences of multiple bonds on the distribution of attachment strengths. Analysis of rupture when multiple bonds are present is nontrivial because partition of the total force amongst the bonds is unknown**.** *How* multiple bonds are loaded depends on topography (roughness) and mechanical compliance at the molecular level - hidden from the observer. The scenario ranges from the load being supported equally by all bonds - *parallel loading* - to the full load being passed between individual bonds in a random sequence of failure - *serial loading* [11]. In *parallel* loading, the force to rupture a contact must reach a level essentially given by the strength of a single bond times the number of bonds. [Note: for *parallel* loading, the apparent rupture peak in the distribution increases more slowly than the number of bonds *n*, i.e. $n^{a/a+1}$.] On the other hand, rupture in *serial* loading will occur at a level close to that for a single bond. These features follow from the stochastic response to increasing loads as shown in Fig. 4b. We see that the likelihood of failure builds up to a peak and quickly approaches complete failure as the load continues to increase -especially for *brittle* bonds. Obviously, less defined loading of multiple bonds broadens the distribution of rupture forces within these limits which makes analysis uncertain even for a few bonds. Surprisingly, the situation may be more tractable because of roughness! The reason is that bonds probably form only at promintories of comparable height along the surface. Hence, aided by local elastic compliance, multiple bonds will tend to support the load in parallel - each experiencing a similar force. In this context, it is important to recognize that all surfaces bearing macromolecules are rough on the mesoscale even if the substrate is atomically smooth.

Assuming that forces of attachment are partitioned equally amongst bonds, the distribution of rupture strengths for a small range of bond formation should approach the convolution of the Poisson-like statistics of assembly with separate distributions for ascending numbers of bonds. This approach was applied to the red cell experiments described in Section 2. Figure 5a shows the optimal correlation of the full statistical convolution with the strength distribution measured for attachments to glycophorin A receptors. Optimization with the frequency of nonattachments either freely variable or fixed at the value indicated by forces in the range of 0 - 20 pN (assumed to be nonspecific) led to identical distributions for strength of specific attachments. The robust fit implied that most of the forces in the 0 - 20 pN bin were nonspecific and that the majority had been detected. By comparison, correlation of the statistical convolution with the strength distribution measured for attachments to glycophorin C receptors was less definitive. In particular, if the frequency of nonattachments was held at the value found in the 0 - 20 pN bin, the correlation was poor as shown in Fig. 5b; but when the frequency of nonattachments was allowed to vary, the correlation was improved significantly (Fig. 5c). However, the value deduced for the frequency of nonattachments was almost an order of magnitude larger than the fraction of forces detected in the 0 - 20 pN bin. Since a stiffer transducer was needed to probe strong attachments in the glycophorin C tests, the implication is that many of the nonspecific forces were mechanically filtered out and not detected. The distributions in Fig. 5 represent the statistical limits expected for large numbers of tests. The result of the deconvolution analysis is to reduce the experimental data to a value of force most likely to rupture single molecular attachments at a particular rate of loading and an exponent *a* that characterizes the intrinsic dependence of the rate of failure on force.

4. Summary

With modest *a priori* assumptions, we have demonstrated that it is possible to isolate the statistical process for bond formation at contact from the dynamic process of rupture subsequent to attachment. The key step is to identify the fraction of contacts that do not result in formation of molecular bonds. Definition of the average likelihood of forming molecular attachments leads to the probability distribution for numbers of bonds involved in attachments. To illustrate the procedure, we examined the use of nonspecific force levels to represent *nonattachments* in tests of point agglutination to red

cell surfaces. However, a more satisfactory diagnostic for contact is to observe the submicroscopic separation at closest approach since nonspecific forces are often too weak to detect reliably. The next step is to convolve a general physical model for rupture of a single attachment under force with the probabilities for numbers of bonds to predict trial distributions for attachment strength. Correlation with the experimental distribution of attachment strengths yields the most probable force for rupture of a single molecular attachment and the exponent *a* that characterizes the dependence of failure rate on load. Surprisingly, the peak exhibited in a distribution of attachment strengths reflects the finite rate of loading and not just discrete bonding in attachments. If experimental distributions are obtained at various loading rates, then the intrinsic parameters, force f_0 and frequency of failure ν_0, that govern strength of attachments at the molecular level can be established as well as a critical test of the general physical prescription for failure kinetics.

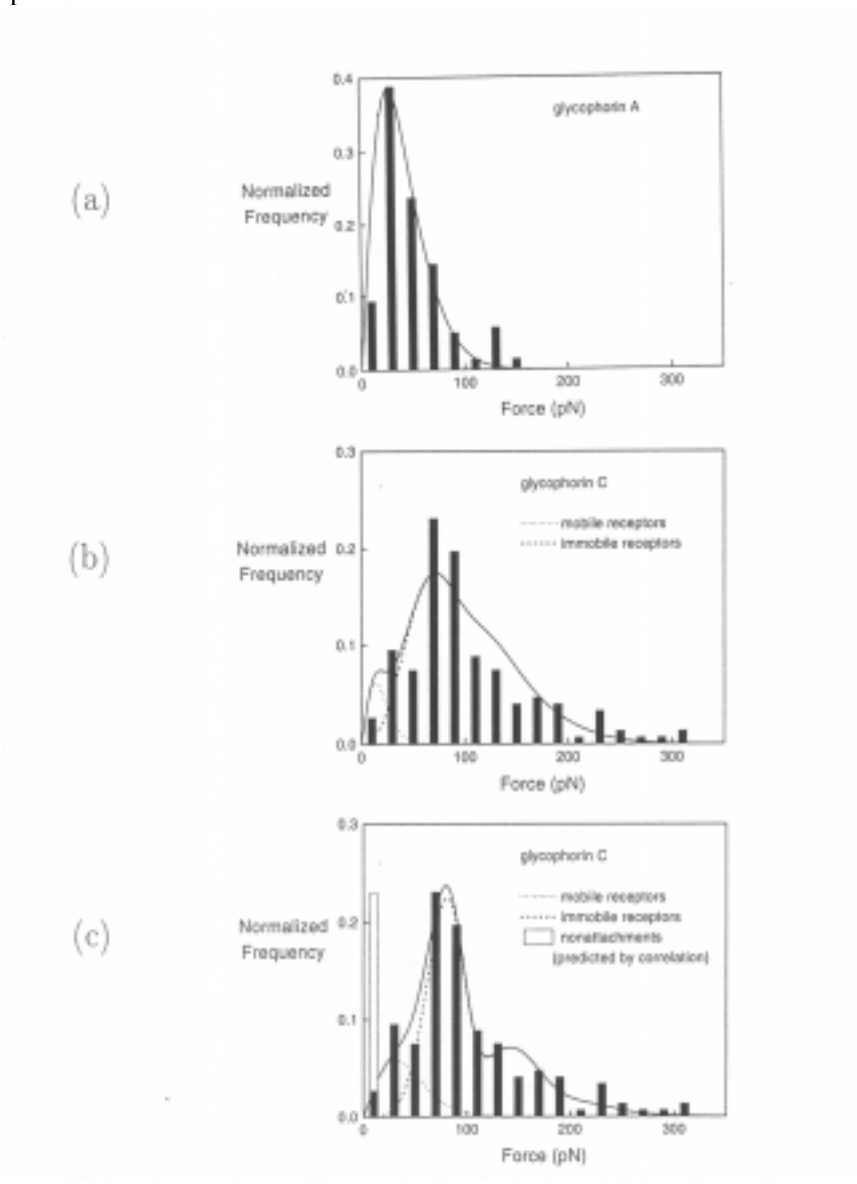

Figure 5. Optimal correlations of the full statistical convolution of bond formation and attachment rupture processes to the data in Fig. 2. In (a) and (b), the correlations were performed assuming that forces measured in the 0-20 pN range represent nonspecific attachments and the likelihood of *zero* bonds in an attachment. The distribution in (c) was found from optimal correlation allowing the frequency of *zero* bonds to vary; the result in (a) was unaffected by this procedure.

Acknowledgement

The authors appreciate the major contributions by Andrew Leung and Susan Tha who carried out the red cell attachment studies. This work was supported by National Science and Engineering Research Council of Canada grant OGPI55415, U.S. National Institutes of Health grant HL31579, and stimulated by the program in *Science of Soft Surfaces and Interfaces* sponsored by the Canadian Institute for Advanced Research.

References

1. Springer TA (1990) Nature 346:425-434

2. Piggot C, Power C (1993) Adhesion Molecule Facts Book. Academic Press, San Diego

3. Lee GU, Kidwell DA, Colton RJ (1994) Langmuir 10:354-357

4. Florin E-L, Moy VT, Gaub HE (1994) Science 264:415-417

5. Leckband DE, Israelachvili JN, Schmitt F-J, Knoll W (1992) Science 255:1419-1421

6. Tees DFJ, Coenen 0, Goldsmith HL (1993) Biophys J 65:1318-1334

7. Evans E, Merkel R, Ritchie K, Tha S, Zilker A (1994) In Laboratory Manual: Methods for Studying Cell Adhesion. Bongrand P, Claesson P, Curtis A (eds). Springer Verlag, Berlin (in press)

8. Bennett V (1990) Physiol Rev 70:1029-1060

9. Narla M, Evans E (1994) Ann Rev Biophys & Biomol Structure 23:787-818

10. Tha S, Leung A, Evans E (to be submitted)

11. Evans E, Berk D, Leung A (1991) Biophys J 59:838-848

12. Evans E (1994) In Biophysics Handbook. Vol. I. Lipowsky R, Sackmann E (eds). Elsevier, Amsterdam (in press)

13. Papoulis, A (1965) Probability, Random Variables, and Stochastic Processes. McGraw-Hill, New York

14. Knowles DW, Chasis JA, Narla M, Evans E (1994) Biophys J 66:1726-

15. Bell GI (1978) Science 200:618-627